MedChemComm

Accepted Manuscript

This article can be cited before page numbers have been issued, to do this please use: G. Wu, Y. gao, D. Kang, B. Huang, Z. Huo, H. Liu, V. Poongavanam, P. Zhan and X. Liu, *Med. Chem. Commun.*, 2017, DOI: 10.1039/C7MD00457E.

ROYAL SOCIETY OF CHEMISTRY

rsc.li/medchemcomm

View Article Online
DOI: 10.1039/C7MD00457E

Design, Synthesis and Biological Evaluation of Tacrine 1,2,3-Triazole Derivatives as Potent Cholinesterase Inhibitors

Gaochan Wu[a], Yun Gao[a], Dongwei Kang[a], Boshi Huang[a], Zhipeng Huo[a], Huiqing Liu[c], Vasanthanathan Poongavanam[b,*], Peng Zhan[a,*], Xinyong Liu[a,*]

[a]*Department of Medicinal Chemistry, Key Laboratory of Chemical Biology (Ministry of Education), School of Pharmaceutical Sciences, Shandong University, 44 West Culture Road, 250012 Ji'nan, Shandong, PR China*

[b]*Department of Physics, Chemistry, and Pharmacy, University of Southern Denmark, DK-5230 Odense M. Denmark.*

[c]*Institute of Pharmacology, School of Medicine, Shandong University, 44, West Culture Road, 250012 Jinan, Shandong, PR China*

***E-mails**: nobelvasanth@gmail.com (Poongavanam V.); zhanpeng1982@sdu.edu.cn (Zhan P.); xinyongl@sdu.edu.cn (Liu X.Y.).

Abstract: We report herein the design and synthesis of a series of 11 novel tacrine-1,2,3-triazole derivatives *via* Cu(I)-catalyzed, alkyne–azide 1,3-dipolar cycloaddition (CuAAC) reaction. The newly synthesized compounds were evaluated for their inhibition activity against electrophorus electricus acetylcholinesterase (AChE) and horse serum butyrylcholinesterase (BChE) as the potential drug targets for Alzheimer's disease (AD). Among the designed compounds, compound **8a2** exhibited the potent inhibition against AChE and BChE with IC_{50} values of 4.89 μM and 3.61 μM, respectively. Further structure-activity relationships (SARs) and molecular modeling studies may serve as valuable insights for the designing of better tacrine-triazole analogues with potential therapeutic applications for the AD.

Introduction

Alzheimer's disease (AD) characterized by a progressive loss of memory and other cognitive function impairments is the most common form of senile dementia.[1] Environmental, genetic and some endogenous factors play a role during the development of AD. Recent study estimates over 36 million people are living with AD worldwide with an estimated global economic impact of approximately $605 billion in 2010,[2] however, the figure has changed to $818 billion in 2015,[3] an increase of 35% since

View Article Online
DOI: 10.1039/C7MD00457E

2010. It has been predicted that if an efficient treatment isn't developed by 2050, the number of patients with AD will rise to 70 million.[4] The impact of this pathology is tremendous for the patients and their families. According to the Alzheimer's Association,[5] AD is the only one without a means to prevent, cure, or slow its progression among the top 10 causes of death in the United States. Although there has been considerable improvement in the management of AD, due to its complex pathogenesis, a successful AD chemotherapy is still demanding and challenging for medicinal chemist. Given the background, several hypotheses have been proposed which include the cholinergic hypothesis.[6-8] This hypothesis suggests that the loss of cholinergic activity is related to the severity of AD.[7] Studies have shown that human acetylcholinesterase (hAChE) or 'pseudocholinesterase' (also called as human butyrylcholinesterase (hBChE) can quickly break down acetylcholine in the body, produce inactive acetic acid and choline, and thereby terminate nerve impulses,[9, 10] which caused the loss of learning ability and cognition. Thus, demoting acetylcholinesterase (AChE) so as to increase the level of acetylcholine (ACh) could be beneficial to alleviate AD's symptoms. Meanwhile, there was evidence showed that butyrylcholinesterase (BChE), a serine hydrolase related to AChE, catalyzed the hydrolysis of esters of choline, including ACh, and played important roles in cholinergic neurotransmission.[11] That is to say, the inhibition of butyrylcholinesterase (BChE) can raise ACh levels. Consequently, dual inhibition of AChE/BChE may be helpful to improve AD symptoms without remarkable side effects.[12] Both hAChE and hBChE structures are very well characterized from X-ray crystallography studies as being small and a narrow gorge structure, mainly composed of the catalytic active site (CAS) at the bottom of the gorge and the peripheral anionic site (PAS) at the entrance of the gorge.[13] In the hAChE, CAS region is mainly composed of the Ser203, Glu334, Trp86, Pro446, Phe295, Phe297, Gly120, Gly121, Ala204 and His447 residues.[14] Among them, catalytic triad (Ser203, Glu334, and His447) mainly involved in the hydrolysis of choline, and PAS region is composed of Asp74, Tyr72, Tyr124, Trp286 and Arg298 residues which stabilize the substrate binding. Although hAChE and hBChE have high homology (54% identity and 81% similarity), the hAChE catalytic gorge is lined by fourteen aromatic residues e.g., Tyr72, Tyr124, Trp286, Phe295, Phe297, and Tyr337, whereas six of these positions were replaced by aliphatic residues (Asn68, Gln119, Ala277, Leu286, Val288, and Ala328) in hBChE.[14] Importantly, π-stacking interaction is the main force in the substrate and inhibitor binding, e.g. tacrine's aromatic ring.

View Article Online
DOI: 10.1039/C7MD00457E

So far, five cholinergic drugs have been approved for clinical use, namely tacrine, donepezil, rivastigmine, galantamine, and huperzine A and many others are in various stages of clinical trials. Among them, tacrine, the first drug approved by FDA that binds at CAS region,[15] is a potent nonselective inhibitor of both hAChE and hBChE and show large modifiable chemical space. Nonetheless, Tacrine suffers from severe side effects including liver toxicity.[16] On the other hand, quinoline derivatives (**I-IV**) [17-20] were reported with specifically binding ability to PAS and displayed favorable anti-AD activity (**Fig. 1**). The purpose of this study was to investigate the effect of dual binding site inhibitors on the PAS and CAS of ChE and to find more effective ChE inhibitors.

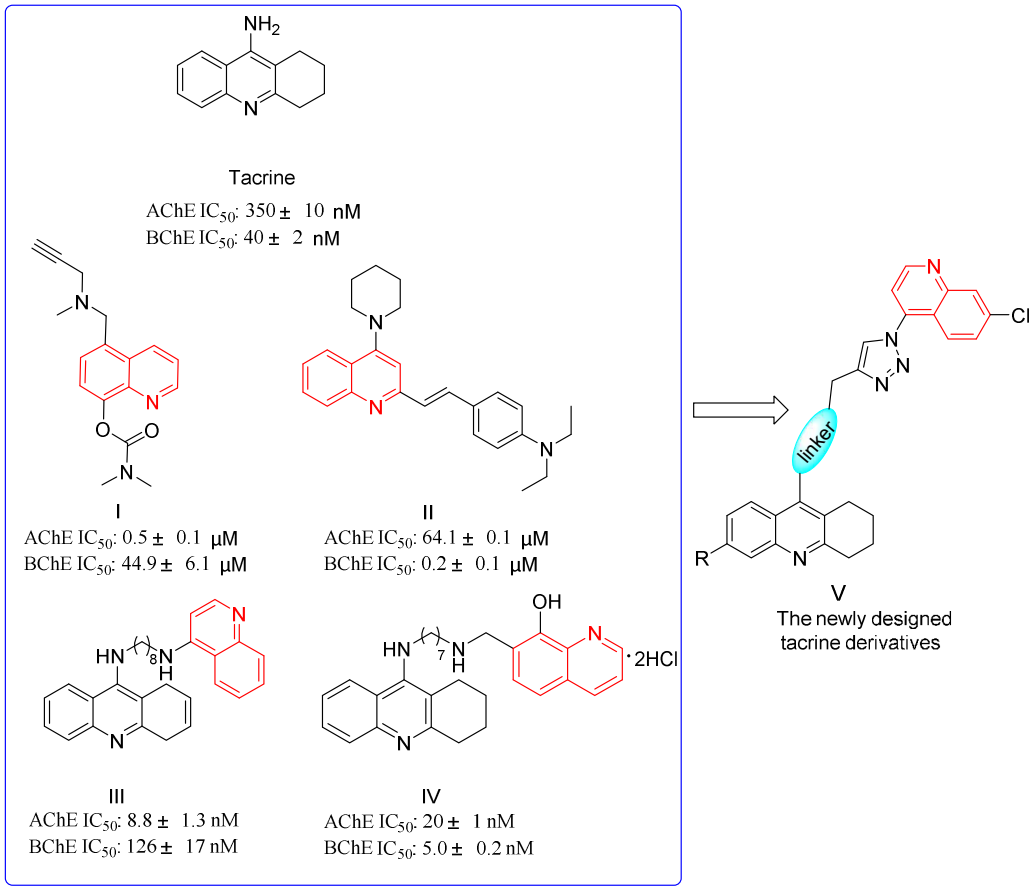

Fig. (1): Tacrine and quinoline derivatives with favorable inhibitory activity, and the newly designed tacrine derivatives.

Meanwhile, conjugation of functional molecules through 1,2,3-triazole have received great attention in drug discovery for the reason that the 1,2,3-triazole structural motif is a neoclassical bioisostere of amide, which is a widely employed functional group in approved drugs.[21] In general,

View Article Online
DOI: 10.1039/C7MD00457E

1,2,3-triazole possessed several advantages in the drug design.[22, 23] For instance, the triazole has two H-bond acceptors which capable of interacting with the biomolecular targets through H-bonding, π-π stacking, and dipole interaction. Besides, triazole ring exhibits better chemical stability in the biological environments, and this improves the pharmacokinetic and toxicity properties. All these advantages made the 1,2,3-triazole become a remarkable fragment in the drug design. Besides, the formation of 1,2,3-triazole compounds *via* Cu(I)-catalyzed, alkyne-azide 1,3-dipolar cycloaddition (CuAAC) reaction, often referred to as click chemistry, is widely used for the rapid assembly of heterocyclic molecules that may be subsequently used as candidate leads in drug development.[24]

Considering the above benefits and in continuation of our interest in searching for the anti-AChE and anti-BChE pharmacological effects of tacrine-based PAS-CAS dual binders, in the present study, we describe the synthesis and evaluation of a set of diverse tacrine-quinolines (See **Figure 1**) as PAS-CAS dual inhibitors for electric eel AChE and horse serum BChE.

Results and discussions

Chemistry

The synthetic route towards the target tacrine-1,2,3-triazole derivatives was outlined in **Scheme 1-3**. Initially, the commercially available starting material indoline-2,3-dione (**1**) yield intermediate 2-aminobenzoic acid (**2a**) in the presence of sodium hydroxide and 30% hydrogen peroxide. Under the presence of $POCl_3$, compound **2a** (or **2b**) reacted with cyclohexanone to obtain 9-chloro-1,2,3,4-tetrahydroacridine (**3a**) or 6,9-dichloro-1,2,3,4-tetrahydroacridine (**3b**), which were used to yield intermediate **4a** (or **4b**, or **4c**) by nucleophilic substitution reaction. Then **4a** (or **4b**, or **4c**) reacted with different fragments of alkyne giving the key intermediates **5a1-5a5** and **5b1-5b6**.[25-29] In the meantime, compound **6** was reacted with NaN_3 in the presence of NaI to prepare compound **7**, which followed by reaction with **5a1-5a5** and **5b1-5b6** to give the target products **8a** and **8b** *via* CuAAC reaction.[30, 31] The newly synthesized compounds were characterized by physicochemical and spectral means, and the consequence of MS and NMR spectral data were found in agreement with the assigned molecular structures.

View Article Online
DOI: 10.1039/C7MD00457E

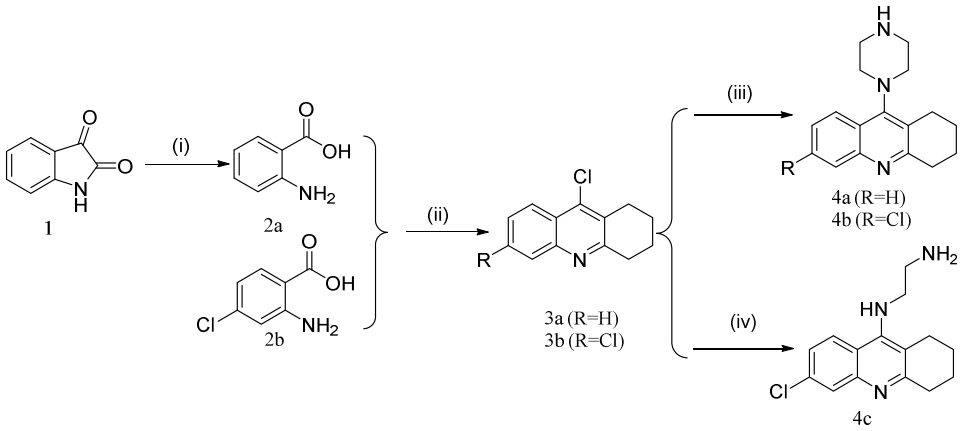

Scheme 1: The synthetic route of intermediates **4a**, **4b** and **4c**. Reagents and Conditions. (i) 30% H_2O_2, NaOH, 0□, 3h; (ii) cyclohexanone, $POCl_3$, 100□, 3h; (iii) piperazine, NaI, PhOH, 180□, 3h; (iv) ethane-1,2-diamine, NaI, PhOH, 180□, 3h.

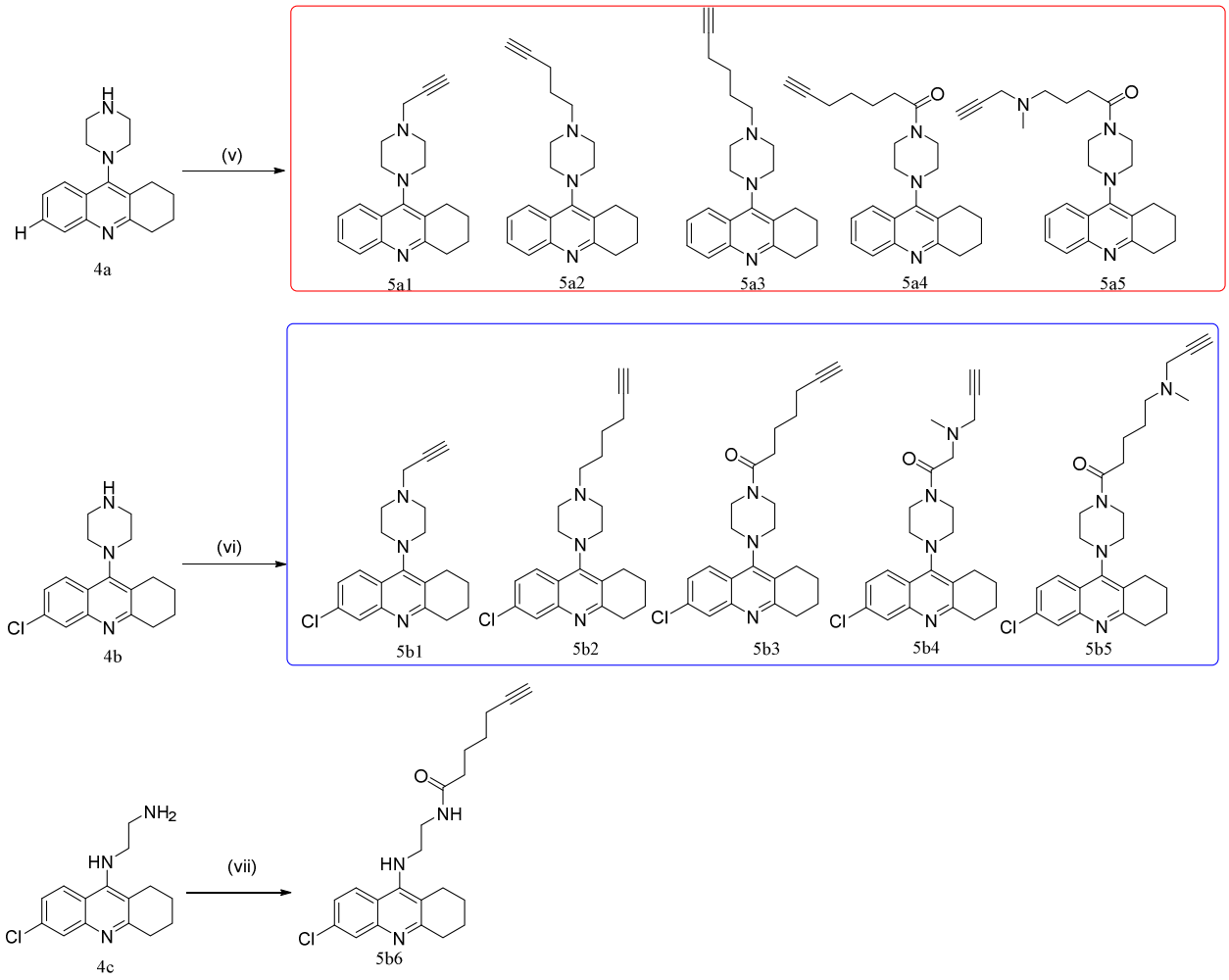

View Article Online
DOI: 10.1039/C7MD00457E

Scheme 2: The synthetic route of intermediates **5a1-5a5** and **5b1-5b6**. Reagents and Conditions. (v) **5a1**: 3-bromoprop-1-yne, Et_3N; **5a2**: 5-chloropent-1-yne, K_2CO_3; **5a3**: 6-chlorohex-1-yne, K_2CO_3; **5a4**: hept-6-ynoic acid, EDCI, HOBt, Et_3N; **5a5**: 1) 4-chlorobutanoyl chloride, Et_3N; 2) N-methylprop-2-yn-1-amine, K_2CO_3; (vi) **5b1**: 3-bromoprop-1-yne, Et_3N; **5b2**: 6-chlorohex-1-yne, K_2CO_3; **5b3**: hept-6-ynoic acid, EDCI, HOBt, Et_3N; **5b4**: 1) 2-chloroacetyl chloride, Et_3N; 2) N-methylprop-2-yn-1-amine, K_2CO_3; **5b5**: 1): 5-bromopentanoyl chloride, Et_3N; 2): N-methylprop-2-yn-1-amine, K_2CO_3; (vii): **5b6**: 1): ethane-1,2-diamine, NaI, PhOH; 2): hept-6-ynoic acid, EDCI, HOBt, Et_3N.

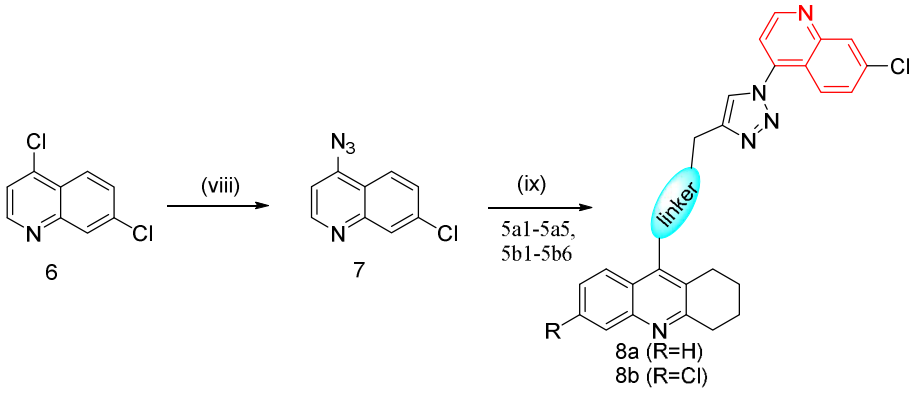

Scheme 3: The synthetic route of tacrine-1,2,3-triazole derivatives. Reagents and Conditions. (viii) NaI, NaN_3, DMF/H_2O (v/v = 1:1), 80□, 8h; (ix) Sodium ascorbate, $CuSO_4$, Et_3N, *n*-butanol/H_2O (v/v = 1:1).

Cholinesterase Inhibition Evaluation

Based on the reported protocol,[32-36] all the newly synthesized compounds (**8a1-8a5**, **8b1-8b6**) were evaluated for their inhibitory activities toward electric eel AChE (Sigma-Aldrich, USA; EC: 3.1.1.7; Product Information File Code: GRO, JWM, RBG, MAM 01/08-1, the download website was shown in the Supporting Information;) and horse serum BChE (Sigma-Aldrich, USA; EC: 3.1.1.8; Product Information File Code: TMG/AJH 10/07, the download website was shown in the Supporting Information;). The authors declare that all procedures were performed in compliance with the Chinese relevant laws and institutional guidelines strictly. Tacrine was selected as a reference drug. The initial *in vitro* screening was performed using single concentration at 100 μM (see Table 1). Among all the tested compounds, compound **8a2** exhibited the most potent inhibitory activity against AChE and BChE with an inhibition ratio of 78.69% and 91.80% at 100 μM. In addition, compounds **8a3**, **8a4**, **8b2**

View Article Online
DOI: 10.1039/C7MD00457E

and **8b3** showed inhibitory percentage for AChE more than 60% at 100 μM, which comparable to that of **8a2**. Interestingly, compound **8b6** had better selectivity for BChE and displayed inhibitory percentage of 82.73% against BChE which about two times than that for AChE (49.37%). After the preliminary screening, compounds **8a2**, **8a3**, **8a4**, **8a5**, **8b2**, **8b3**, and **8b6** were chosen to determine their IC_{50} values for cholinesterase. Among them, **8a2** was demonstrated the best anti-AChE (IC_{50} = 4.89 μM) and anti-BChE activity (IC_{50} = 3.61 μM). Besides, the inhibitory efficacy of **8a3**, **8a4**, **8b3**, and **8b2** demonstrated IC_{50} values against AChE were 10, 11.07, 18.66 and 19.59 μM, respectively. As for anti-BChE activity, **8b6** was inferior to **8a2,** and its IC_{50} value was 6.06 μM, followd by **8a5** (IC_{50} = 61.13 μM) and **8a3** (IC_{50} = 66.68 μM). However, all the newly synthesized compounds showed weaker inhibitory activity compared to the reference drug tacrine.

Preliminary structure-activity relationship (SAR) analysis indicated that the size and length of the linker between the piperazine and triazole motif is a major determinant for their inhibitory activity. An alkane chain with three carbons was the most active one (**8a2**), whether increasing or shortening the length of the carbon chain would decrease their inhibitory effect for AChE and BChE (Inhibition activity: **8a2** > **8a3** > **8a1**). Compared series **a** with series **b**, introducing chlorine atom at the C_6 position of tacrine would decrease the inhibitory activity (Inhibition activity: **8a1** > **8b1**, **8a3** > **8b2**, **8a4 > 8b3**). Current SAR will provide additional information to help in the design of inhibitors with better potency.

Table 1: Inhibition activity of Tacrine derivatives for electrophorus electricus AChE and horse serum BChE.

Compound	R	Linker	Inhibition (%) at 100 μM		IC_{50} (μM)	
			AChE	BChE	AChE	BChE
8a1	H	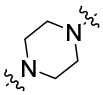	39.32	38.56	-	-
8a2	H	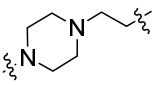	78.69	91.80	4.89	3.61

View Article Online
DOI: 10.1039/C7MD00457E

8a3	H	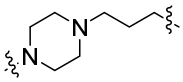	69.31	55.64	10	66.68
8a4	H	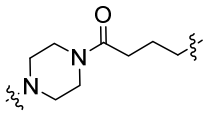	65.69	46.37	11.07	>100
8a5	H	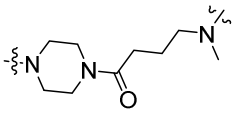	47.56	57.90	>100	61.13
8b1	Cl	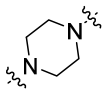	30.38	22.12	-	-
8b2	Cl	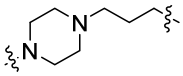	66.02	46.68	19.59	>100
8b3	Cl	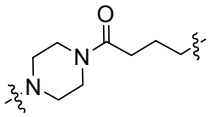	64.19	49.28	18.66	>100
8b4	Cl	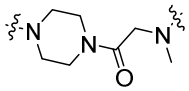	41.47	27.97	-	-
8b5	Cl	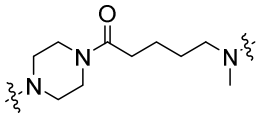	42.31	39.04	-	-
8b6	Cl	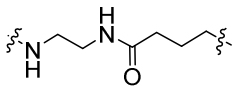	49.37	82.73	>100	6.06
Tacrine	-	-	86.22	99.63	0.316	0.066

Molecular Modeling Analysis

To provide better insight into the binding mode of compound **8a2** to hAChE and hBChE, molecular docking followed by MM-GBSA studies were performed. To this end, compound **8a2** was docked into the hAChE and hBChE ligand-binding site (see experimental section for detail). The active site of hAChE has previously been well characterized as having the catalytic site (CAS), which is composed of the Trp86, Glu334, Tyr336, Trp439, Met443, Pro446 and His447 residues and the

View Article Online
DOI: 10.1039/C7MD00457E

peripheral site or anionic subsite (PAS) which is composed of Asp74, Tyr72, Tyr124, Trp286 and Arg298 residues. It is shown in the crystal structure of hAChE complex with tacrine that the acridine ring involved in the π-π interaction with indole ring of Trp84. In addition to acridine ring surrounded by the hydrophobic residues such as Phe330, Tyr334, Tyr442 and Trp434.[37] The active site of hBChE is very similar as hAChE as having similar set of residues in both CAS and PAS regions.[38] In this study, the binding mode of compound **8a2** is compared in both hAChE and hBChE active site with Tacrine. MM-GBSA method was employed to rank the best-ranked binding pose from the docking solutions, and the binding pose that has shown the highest binding affinity in the MM-GBSA calculation for hAChE and hBChE is further discussed. It is clear from **Fig. 2** that the **8a2** binding mode is similar in both cases and that the acridine ring involved in π-π interaction with Trp86 (hAChE) and Trp82 (hBChE) as it has previously been shown.[37]

Moreover, piperazine and triazole rings of **8a2** compound showed the interaction with Tyr124 and Trp286 in the hAChE. However, compound **8a2** binds slightly better in the hBChE structure, for instance, quinoline ring strongly binds to Ser287 and Pro285 residues through π-π interactions, and importantly, electronegative chlorine atom also shows strong interaction with neighboring residue e.g., Gln71. Besides, tacrine structure also was prepared in the same manner as compound **8a2** and re-docked into hAChE and hBChE active site to assess the docking protocol and compared the binding pose to x-ray crystal structure. Overall, the docking simulation is able to reproduce the same binding pose as it was observed in the x-ray crystallophay with an RMSD of 0.05 A (cf. Figure 2 and supporting information). In addition to the comparison of **8a2** with tacrine, the binding mode of compound III and IV (cf. Figure 1) was compared to understand an impact of linker fragment. The compounds III and IV were also docked same as Tacrine into hAChE and hBChE structures. As clearly seen from the Fig 2C, the binding mode of **8a2** found to be similar as compound III and IV (see protein-ligand interaction map in the Supporting Information) but showed lesser potency as compared to tacrine or compound III/IV. The higher IC_{50} of **8a2** could be due to not only rigid triazole and piperazine rings, but also having more polar atoms, which may lead to an unfavorable contribution to the hydrophobicity of active sites, particularly PAS as reported previously.[17,18]

View Article Online
DOI: 10.1039/C7MD00457E

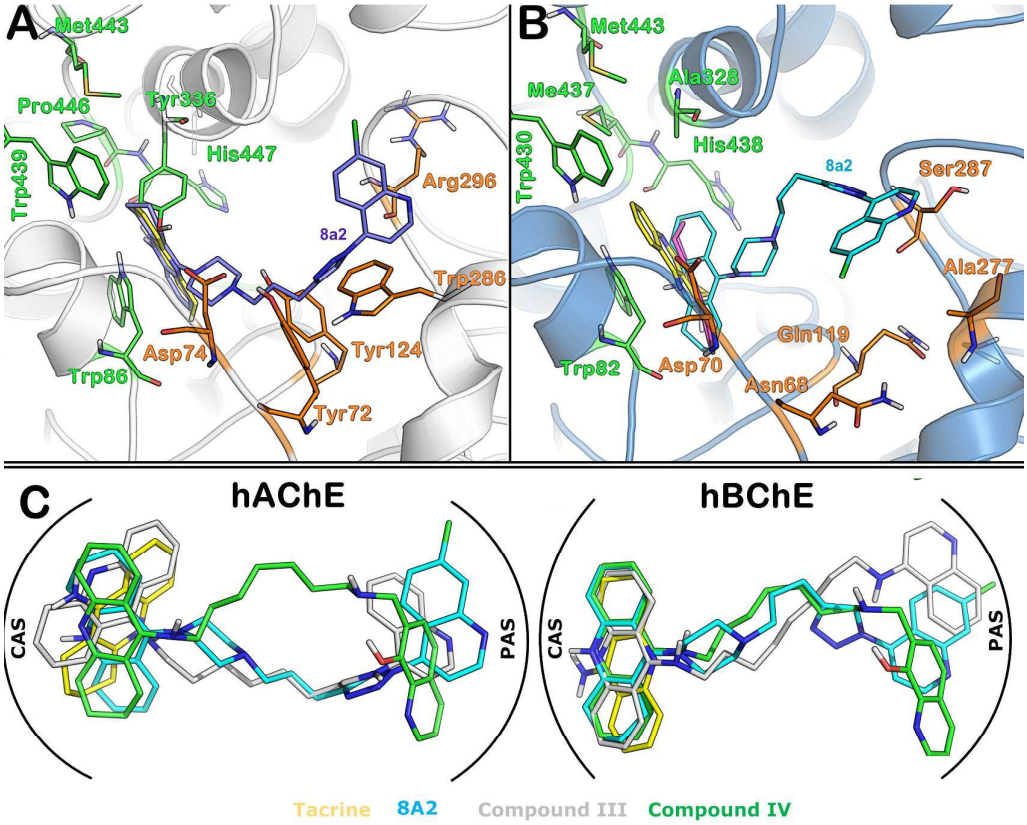

Fig. (2): Comparison of the binding mode of compound **8a2** (cyan) at the active site of hAChE (A) and hBChE (B). Important residues belonging to CAS (green) and PAS (orange) are highlighted. Schematic representation of binding poses of **8a2** with compounds III, IV and tacrine (for clarity only ligand pose is shown).

Conclusion

To summarize, a concise and efficient synthetic approach has been established to readily access two novel series of tacrine-1,2,3-triazole derivatives in moderate to high yields. Subsequently, the synthesized compounds were screened for electric eel AChE and horse serum BChE inhibition. Among these compounds, compound **8a2** inhibited the AChE and horse serum BChE activity by more than 75% (IC_{50}: 4.89 μM) and 90% (IC_{50}: 3.61 μM) at a concentration of 100 μM, respectively. Although, compound **8a2** inhibits cholinesterase slightly lower as compared to reference drug Tacrine, with its unique binding mode at both at CAS and PAS sites, making it particularly promising lead for the development of new dual inhibitors of AChE and BChE. Further, molecular docking studies were also performed to understand its binding mode in the AChE and BChE active, particularly revealing the

View Article Online
DOI: 10.1039/C7MD00457E

importance of quinoline substituents on the C-1 position of the 1,2,3-triazole ring involved in the π-π interaction with Trp286 (hAChE), Ser287 (hBChE) and Pro285 (hBChE) at PAS region. Meanwhile, the acridine ring involved in π-π interaction with Trp86 (hAChE) and Trp82 (hBChE) at CAS region same as the reference compound Tacrine.

Several works have reported on designing of tacrine-based dimers with different linkers (e.g. disulfide bond, alkane, piperazine, amide etc.), including dual binding site inhibitors on the PAS and CAS towards AChE and BChE, which is a promising trend deserved to be explored and studied.[39] In this work, we take advantages of CuAAC click chemistry in drug design and 1,2,3-triazole unique physiochemical property, thus, adapted a linker including 1,2,3-triazole group introduced by CuAAC reaction but maintained its unique binding mode like Tacrine-based dimers. Although a most potent compound from this series is significantly weaker as compared to Tacrine or previously known compounds e.g., **III** and **IV**, a non-aliphatic linker designing provides further opportunities to design smarter linker which facilitates the molecules to be able to bind to CAS and PAS sites. With this understanding, efforts are further expanded in our laboratory for further lead optimization of Tacrine-based triazole analogues as potent cholinesterase inhibitors with the hope to develop promising candidates for AD chemotherapy.

Experimental Section

General

All melting points of the compounds were determined on a micro melting point apparatus and were uncorrected. ^{1}H-NMR and ^{13}C-NMR spectra were obtained *via* a Bruker Avance-400 NMR-spectrometer in $CDCl_3$. Chemical shifts were expressed in δ units and TMS as internal reference. Mass spectra was conducted *via* a LC Autosampler Device: Standard G1313A instrument. Flash column chromatography was performed on column packed with Silica Gel 60 (200-300 mesh). Meanwhile, TLC was taken on Silica Gel GF254 for TLC and spots were visualized by irradiation with UV light (λ = 254 nm). Solvents were of reagent grade, which were purified and dried by standard methods when necessary. Concentration of the reaction solutions was used the rotary evaporator under reduced pressure condition.

General Procedure for the Synthesis of Compound 7 (4-azido-7-chloroquinoline).

View Article Online
DOI: 10.1039/C7MD00457E

4,7-Dichloroquinoline (**6**, 3.0 g, 11.4 mmol), NaN_3 (2.0 g, 30.0 mmol), and NaI (0.2 g, 1.5 mmol) were dissolved in the solvent of DMF/H_2O (v:v = 1:1, 60 mL). The resulting mixture was stirred at 80□ for 8 h. After the reaction was cooled to the room temperature, water (30 mL) was added to the reaction system. Then the resulting mixture was extracted with ethyl acetate (3 × 40 mL). The combined organic phase was washed with saturated salt water (3 × 40 mL), dried over anhydrous Na_2SO_4, filtered, and concentrated under reduced pressure to give the corresponding crude target product, which was purified by flash column chromatography with petroleum ether/ethyl acetate to afford compound **7** as white solid with the yield of 91%.

General Procedure for the Synthesis of 3a (9-chloro-1,2,3,4-tetrahydroacridine) and 3b (6,9-dichloro-1,2,3,4-tetrahydroacridine).

Indoline-2,3-dione (**1**, 5.0 g, 34.0 mmol) was dissolved in the solvent of NaOH (67 mL, 1 mol/L). After hydrogen peroxide (7.3 mL, 30%) was added into the above solution slowly at 0□, the resulting mixture was stirred at 30-40□ for 3 h. Then the cooling solution was neutralized to pH = 7.5 with hydrochloric acid (3 mol/L). Subsequently, moderate activated carbon was added and stirred for another 0.5 h. Then the resulting precipitate was filtered and further the filtrate was acidized until pH = 4-5 and stirring was continued for another 1 h. The resulting mixture was filtered again and combined with the filter cake, which was dried in the vacuum drying oven to obtain the crude product **2a**. The crude product **2a** was purified by flash column chromatography with dichloromethane/methanol to afford compound **2a** as white hairy solid with the yield of 84%.

2-Aminobenzoic acid (**2a**, 1.0 g, 7.3 mmol) and cyclohexanone (0.9 g, 8.8 mmol) were mixed in the flask. Then $POCl_3$ (10 mL) was added dropwise into the flask at 0□. The above resulting mixture was refluxed at 100□ for 3 h. Then the mixture was quenched with ice water and neutralized to neutral with K_2CO_3 solution (1 mol/L). Subsequently, the neutralized solution was extracted with ethyl acetate (3 × 15 mL), and the combined organic phase was washed with saturated salt water (3 × 15 mL), dried over anhydrous $MgSO_4$, filtered, and concentrated under reduced pressure to give the corresponding crude target product. Finally, crude product was purified by flash column chromatography with petroleum ether/ethyl acetate to afford product compound **3a** as yellow solid. Yield: 88%. To be noted, synthetic operation of compound **3b** (Yellow solid; Yield: 81.5%) was also the same to compound **3a**.

General Procedure for the Synthesis of compound 4a (9-(piperazin-1-yl)-1,2,3,4-tetrahydroacridine),

View Article Online
DOI: 10.1039/C7MD00457E

4b (6-chloro-9-(piperazin-1-yl)-1,2,3,4-tetrahydroacridine) and 4c (N1-(6-chloro-1,2,3,4-tetrahydroacridin-9-yl) ethane-1,2-diamine).

Compound **3a** (or **3b**, 13.8 mmol), piperazine (5.9 g, 69.0 mmol), NaI (0.2 g, 13.8 mmol) and phenol (2.6 g, 27.6 mmol) were mixed and stirred at 180□ for 3 h in the flask. Then the reaction system was cooled to 80□ and subsequently quenched with NaOH solution (30 mL, 1 mol/L). The quenched mixture was extracted with dichloromethane (3 × 15 mL), and the combined organic phase was washed with saturated salt water (3 × 15 mL), dried over anhydrous Na_2SO_4, filtered, and concentrated under reduced pressure to give the corresponding crude target product, which was purified by flash column chromatography with dichloromethane/methanol to afford compound **4a** (**4b**) as yellow solid (yellow oil) with the yield of 81% (42%). The same procedure was used to obtain product **4c** with yield of 82%, only with the difference that the piperazine was changed to ethane-1,2-diamine.

General Procedure for the Synthesis of compound 5a1-3 and 5b1-2.

Compound **4a** (**4b**, 3.7 mmol), 3-bromoprop-1-yne (0.49 g, 4.1 mmol), and triethylamine (0.6 g, 5.6 mmol) were stirred at 50□ for 3 h in the solvent of dichloromethane. Then the reaction mixture was cooled to the room temperature and concentrated under the reduced pressure to obtain the crude product, which was purified by flash column chromatography with dichloromethane/methanol to get compound **5a1** (**5b1**) as yellow solid (yellow solid). Yield: 70% (82%). If 3-bromoprop-1-yne was changed to 5-chloropent-1-yne or 6-chlorohex-1-yne, **5a2**, **5a3**, and **5b2** would be obtained with yield of 81%, 69% and 49%, respectively.

General Procedure for the Synthesis of compound 5a4, 5b3 and 5b6.

Hept-6-ynoic acid (0.5 g, 4.0 mmol), EDCI (1.0 g, 5.0 mmol), and HOBt (0.7 g, 5.0 mmol) were stirred at room temperature for 0.5 h in dichloromethane. Then compound **4a** (**4b** or **4c**, 3.3 mmol,) and triethylamine (0.7 g, 6.6 mmol) were added, and the reaction was continued at the room temperature for another 5 h. Once the reaction was finished (monitored by TLC), the reaction mixture was quenched with saturated salt water (3 × 30 mL), dried over anhydrous $MgSO_4$, filtered, and concentrated under reduced pressure to give the corresponding crude target product, which was purified by flash column chromatography with dichloromethane/methanol to get compound **5a4** (**5b3** or

View Article Online
DOI: 10.1039/C7MD00457E

5b6) as yellow solid. Yield: 50% (70% or 86%).

General Procedure for the Synthesis of compound 5a5, 5b4, 5b5, and 5b6.

4-chlorobutanoyl chloride (0.8 g, 5.6 mmol) was added dropwise into the solvent of dichloromethane (25 mL) at 0□, which previously stirred with triethylamine (0.7 g, 7.4 mmol) and compound **4a** (1.0 g, 3.7 mmol). Then the reaction was continued at 0□ under magnetic stirring for 0.5 h. Subsequently, stirring was continued for another 2 h at room temperature. Once the reaction was completed (monitored by TLC), the resulting mixture was washed with saturated salt water (3 × 25 mL), dried over anhydrous $MgSO_4$, filtered, and concentrated under reduced pressure to give the corresponding crude target product, which was purified by flash column chromatography with petroleum ether/ethyl acetate to obtain the precursor of compound **5a5**. Yield: 82%. And then compound **5a5** reacted with *N*-methylprop-2-yn-1-amine as the synthetic operation of compound **4a**, **4b** and **4c**, and was purified by flash column chromatography. Yellow solid. When the same procedure, only with the difference that procedure 4-chlorobutanoyl chloride was changed to 2-chloroacetyl chloride or 5-bromopentanoyl chloride, product **5b4** and **5b5** were obtained with yield of 83% and 89%, respectively.

General Procedure for the Synthesis of compound 8a1-8a5 and 8b1-8b6.

Intermediate **5a1-5a5** (1.0 eq, or **5b1-5b6)**, 4-azido-7-chloroquinoline (compound **7**, 1.0 eq), ascorbic acid sodium (0.6 eq), $CuSO_4.5H_2O$ (0.3 eq) and triethylamine (1.2 eq) were dissolved in the solution of *n*-butyl alcohol/water (v:v = 1:1). The resulting mixture was stirred at room temperature for 5 h. Then the reaction mixture was extracted with ethyl acetate (3 × 10 mL), and the combined organic phase was washed with saturated salt water (3 × 10 mL), dried over anhydrous $MgSO_4$, filtered, and concentrated under reduced pressure to give the corresponding crude target product, which was purified by flash column chromatography to afford product **8a1-8a5** (or **8b1-8b6**). Yield: 37%-92%.

9-(4-((1-(7-chloroquinolin-4-yl)-1H-1,2,3-triazol-4-yl)methyl)piperazin-1-yl)-1,2,3,4-tetrahydroacridine (8a1). Yield: 74%; White solid; mp:105-107°C. ^{1}H NMR (400 MHz, $CDCl_3$, ppm) δ: 9.08 (d, *J* = 4.6 Hz, 1H), 8.26 (d, *J* = 2.0 Hz, 1H), 8.16 (d, *J* = 8.0 Hz, 1H), 8.07-8.05 (m, 2H), 7.97 (d, *J* = 8.3 Hz, 1H), 7.64-7.57 (m, 2H), 7.54 (d, *J* = 4.6 Hz, 1H), 7.42 (t, *J* = 7.2 Hz, 1H), 3.99 (s, 2H), 3.41 (s, 4H), 3.13 (t, *J* = 6.6 Hz, 2H), 2.96-2.87 (m, 6H), 1.97-1.82 (m, 4H); ^{13}C NMR (100 MHz, $CDCl_3$, ppm) δ:

View Article Online
DOI: 10.1039/C7MD00457E

160.3, 152. 8, 151.4, 150.3, 147. 7, 145.6, 141.1, 137.0, 129.5, 129.1, 128.7, 128.4, 127.7, 125.8, 125.1, 124.7, 124.5, 123.9, 120.6, 115.8, 54.4, 53.7, 50.4, 34.0, 26.9, 23.0, 22.8. ESI-MS: $C_{29}H_{28}ClN_7$, Exact Mass: 509.21, m/z 511.5 $(M + 2)^+$.

9-(4-(3-(1-(7-chloroquinolin-4-yl)-1H-1,2,3-triazol-4-yl)propyl)piperazin-1-yl)-1,2,3,4-tetrahydroacridine (8a2). Yield：47%; White solid; mp: 98-100°C. ^{1}H NMR (400 MHz, $CDCl_3$, ppm) δ: 9.03 (d, *J* = 4.6 Hz, 1H), 8.22 (d, *J* = 2.0 Hz, 1H), 8.15 (d, *J* = 8.0 Hz, 1H), 8.04 (d, *J* = 9.1 Hz, 1H), 7.95 (d, *J* = 8.3 Hz, 1H), 7.86 (s, 1H), 7.59-7.54 (m, 2H), 7.48 (d, *J* = 4.6 Hz, 1H), 7.40 (t, *J* = 7.6 Hz, 1H), 3.37 (s, 4H), 3.11 (t, *J* = 6.6 Hz, 2H), 3.01-2.92(m, 4H), 2.72-2.63 (m, 6H), 2.14 -2.06 (m, 2H), 1.96 -1.80 (m, 4H)；^{13}C NMR (100 MHz, $CDCl_3$, ppm) δ: 160.3, 152.8, 151.4, 150.2, 148.7, 147.8, 141.1, 136.6, 129.2, 128.9, 128.7, 128.3, 127.6, 125.9, 124.9, 124. 8, 123.9, 122.6, 120.5, 115.8, 58.2, 54.3, 50.5, 34.1, 26.9, 26.5, 23.5, 23.0, 22.8. ESI-MS: $C_{31}H_{32}ClN_7$, Exact Mass: 537.24, m/z 539.2 $(M + 2)^+$.

9-(4-(4-(1-(7-chloroquinolin-4-yl)-1H-1,2,3-triazol-4-yl)butyl)piperazin-1-yl)-1,2,3,4-tetrahydroacridine (8a3). Yield: 43%; White solid; mp:112-115 °C. ^{1}H NMR (400 MHz, $CDCl_3$, ppm) δ: 9.05 (d, *J* = 4.6 Hz, 1H), 8.24 (d, *J* = 2.0 Hz, 1H), 8.15 (d, *J* = 8.3 Hz, 1H), 8.06-8.00 (m, 2H), 7.83 (s, 1H), 7.61-7.56 (m, 2H), 7.50 (d, *J* = 4.6 Hz, 1H), 7.41 (t, *J* = 7.6 Hz, 1H), 3.38 (s, 4H), 3.15 (t, *J* = 6.6 Hz, 2H), 2.98-2.92 (m, 4H), 2.72 (s, 4H), 2.61-2.57 (m, 2H),1.97-1.72 (m, 8H); ^{13}C NMR (100 MHz, $CDCl_3$, ppm) δ: 160.3, 153.1, 151. 6, 150.3, 149.0, 147.5, 141.2, 136.8, 129.3, 129.0, 128.6, 128.4, 127.6, 125.9, 125.0, 124.8, 124.0, 122. 6, 120.7, 115.8, 58.7, 54.4, 50.4, 34.1, 27.3, 26.9, 26.5, 25.5, 23.0, 22.8. ESI-MS: $C_{32}H_{34}ClN_7$, Exact Mass: 551.26, m/z 553.2 $(M + 2)^+$.

5-(1-(7-chloroquinolin-4-yl)-1H-1,2,3-triazol-4-yl)-1-(4-(1,2,3,4-tetrahydroacridin-9-yl)piperazin-1-yl)pentan-1-one (8a4). Yield: 64%; White solid; mp: 98-101°C. ^{1}H NMR (400 MHz, $CDCl_3$, ppm) δ 9.03 (d, *J* = 4.6 Hz, 1H), 8.21 (d, *J* = 2.0 Hz, 1H), 8.09-8.03 (m, 2H), 7.97-7.91 (m, 2H), 7.61-7.55 (m, 2H), 7.49 (d, *J* = 4.6 Hz, 1H), 7.43 (t, *J* = 7.6 Hz, 1H), 4.08-3.71 (m, 4H), 3.33-3.28 (m, 4H), 3.12 (t, *J* = 6.5 Hz, 2H), 2.98-2.89 (m, 4H), 2.52 (t, *J* = 7.0 Hz, 2H), 1.97-1.82 (m, 8H); ^{13}C NMR (100 MHz, $CDCl_3$, ppm) δ: 171.4, 160.6, 152.0, 151.4, 150.2, 148.8, 147.8, 141.1, 136.7, 129.2, 129.0, 128. 9, 128. 5, 127.9, 125.8, 125.3, 124.8, 123.4, 122.7, 120.6, 115.8, 50.6, 50.2, 46.8, 42.8, 34.1, 32.9, 28.9, 26.8, 25.4, 24.7, 22.9, 22.7. ESI-MS: $C_{33}H_{34}ClN_7O$, Exact Mass: 579.25, m/z 581.5 $(M + 2)^+$.

4-(((1-(7-chloroquinolin-4-yl)-1H-1,2,3-triazol-4-yl)methyl)(methyl)amino)-1-(4-(1,2,3,4-tetrahydroacridin-9-yl)piperazin-1-yl)butan-1-one (8a5). Yield: 43%; White solid; mp:110-112°C. ^{1}H NMR (400

View Article Online
DOI: 10.1039/C7MD00457E

MHz, $CDCl_3$, ppm) δ: 9.05 (d, *J* = 4.3 Hz, 1H), 8.23 (d, *J* = 1.7 Hz, 1H), 8.08-8.04 (m, 3H), 7.96 (d, *J* = 8.3 Hz, 1H), 7.61-7.57 (m, 2H), 7.54 (d, *J* = 4.6 Hz, 1H), 7.42 (t, *J* = 7.5 Hz, 1H), 3.91-3.70 (m, 6H), 3.31-3.25 (m, 4H), 3.12 (t, *J* = 6.5 Hz, 2H), 2.89 (t, *J* = 6.2 Hz, 2H), 2.62-2.41 (m, 7H), 2.03-1.83 (m, 6H); ^{13}C NMR (100 MHz, $CDCl_3$, ppm) δ: 171.4, 160.5, 152.0, 151.4, 150.2, 147.9, 145.8, 141.1, 137.0, 129.4, 129.0, 128.5, 127. 9, 125.8, 125.3, 124. 8, 124.5, 123.4, 120.6, 116.0, 56.3, 52.0, 50.7, 50.2, 46.8, 42.8, 42.6, 34.1, 30.7, 26.8, 22.93, 22.7. ESI-MS: $C_{34}H_{37}ClN_8$, Exact Mass: 608.28, m/z 609.4 $(M + 1)^+$.

6-Chloro-9-(4-((1-(7-chloroquinolin-4-yl)-1H-1,2,3-triazol-4yl)methyl)piperazin-1-yl)-1,2,3,4-tetrahydroacridine (8b1). Yield: 92%; Yellow solid; mp:115-117°C. ^1H NMR (400 MHz, $CDCl_3$, ppm) δ: 9.08 (d, *J* = 4.6 Hz, 1H), 8.26 (d, *J* = 1.9 Hz, 1H), 8.10-8.04 (m, 3H), 7.96 (d, *J* = 1.6 Hz, 1H), 7.63 (dd, *J* = 9.1, 2.0 Hz, 1H), 7.53 (d, *J* = 4.6 Hz, 1H), 7.36 (dd, *J* = 9.0, 2.0 Hz, 1H), 3.99 (s, 2H), 3.39 (s, 4H), 3.11 (t, *J* = 6.6 Hz, 2H), 2.94-2.88 (m, 6H), 2.88 (s, 4H), 1.97-1.82 (m, 4H); ^{13}C NMR (100 MHz, $CDCl_3$, ppm) δ: 161.8, 152.8, 151.4, 150.3, 148.3, 145.6, 141.0, 137.0, 134.1, 129.4, 129.1, 127.9, 127.7, 125.9, 125.4, 124.7, 124.5, 124.3, 120.6, 115.9, 54.3, 53.6, 50.4, 34.1, 26.9, 22.9, 22.7. ESI-MS: $C_{29}H_{27}Cl_2N_7$, Exact Mass: 543.17, m/z 545.2 $(M + 2)^+$.

6-Chloro-9-(4-(4-(1-(7-chloroquinolin-4-yl)-1H-1,2,3-triazol-4-yl)butyl)piperazin-1-yl)-1,2,3,4-tetrahydroacridine (8b2). Yield: 52.6%; White solid; mp:128-130°C. ^1H NMR (400 MHz, $CDCl_3$, ppm) δ: 8.87 (d, *J* = 4.6 Hz, 1H), 8.05 (d, *J* = 1.8 Hz, 1H), 7.95-7.9 (m, 2H), 7.76 (s, 2H), 7.42 (dd, *J* = 9.1, 2.0 Hz, 1H), 7.34 (d, *J* = 4.6 Hz, 1H), 7.17 (dd, *J* = 9.0, 1.9 Hz, 1H), 3.20 (s, 4H), 2.93 (t, *J* = 6.5 Hz, 2H), 2.83 (t, *J* = 7.6 Hz, 2H), 2.77 (t, *J* = 6.2 Hz, 2H), 2.56-2.42 (m, 4H), 1.83-1.59 (m, 8H); ^{13}C NMR (100 MHz, $CDCl_3$, ppm) δ: 161.6, 152.8, 151.3, 150.1, 148.8, 148.0, 141.0, 136.6, 133. 8, 129.1, 128.8, 127.8, 127.5, 125.6, 125.5, 124.8, 124.2, 122.5, 120.5, 115. 7, 58.6, 54.2, 50.4, 34.0, 27.3, 26. 8, 26.5, 25.5, 22.8, 22.6. ESI-MS: $C_{32}H_{33}Cl_2N_7$, Exact Mass: 585.22, m/z 586.9 $(M + 1)^+$.

1-(4-(6-Chloro-1,2,3,4-tetrahydroacridin-9-yl)piperazin-1-yl)-5-(1-(7-chloroquinolin-4-yl)-1H-1,2,3-triazol-4-yl)pentan-1-one (8b3). Yield: 80%; Yellow solid; mp:108-110°C. ^1H NMR (400 MHz, $CDCl_3$, ppm) δ: 9.06 (d, *J* = 4.6 Hz, 1H), 8.24 (d, *J* = 1.9 Hz, 1H), 8.06-8.0 (m, 3H), 7.87 (s, 1H), 7.60 (dd, *J* = 9.1, 2.0 Hz, 1H), 7.50 (d, *J* = 4.6 Hz, 1H), 7.38 (dd, *J* = 9.0, 2.0 Hz, 1H), 3.72 (s, 4H), 3.32-3.28 (m, 4H), 3.13 (t, *J* = 6.4 Hz, 2H), 2.96 (t, *J* = 7.0 Hz, 2H), 2.89 (t, *J* = 6.3 Hz, 2H), 2.52 (t, *J* = 7.0 Hz, 2H), 1.97-1.84 (m, 8H); ^{13}C NMR (100 MHz, $CDCl_3$, ppm) δ: 171.4, 161.7, 152.3, 151.3, 150.3, 148.6,

View Article Online
DOI: 10.1039/C7MD00457E

148.0, 141.1, 136.8, 134.4, 129.3, 129.0, 128.1, 127. 8, 126.3, 125.0, 124.2, 122.7, 115.8, 50.7, 50.3, 46.8, 42.7, 34.0, 32.9, 28.9, 26.8, 25.3, 24.6, 22.8, 22.6. ESI-MS: $C_{33}H_{33}Cl_2N_7O$, Exact Mass: 613.21, m/z 615.4 $(M + 2)^+$.

1-(4-(6-Chloro-1,2,3,4-tetrahydroacridin-9-yl)piperazin-1-yl)-2-(((1-(7-chloroquinolin-4-yl)-1H-1,2,3-triazol-4-yl)methyl)(methyl)amino)ethan-1-one (8b4). Yield: 70%; White solid; mp:113-116 °C. ^{1}H NMR (400 MHz, $CDCl_3$, ppm) δ: 9.06 (d, *J* = 4.6 Hz, 1H), 8.24 (d, *J* = 2.0 Hz, 1H), 8.14 (s, 1H), 8.09-8.02 (m, 2H), 7.94 (d, *J* = 2.0 Hz, 1H), 7.59 (dd, *J* = 9.1, 2.1 Hz, 1H), 7.53 (d, *J* = 4.6 Hz, 1H), 7.35 (dd, *J* = 9.0, 2.1 Hz, 1H), 4.01 (s, 2H), 3.97-3.49 (m, 4H), 3.44 (s, 2H), 3.30 (d, *J* = 29.1 Hz, 4H), 3.09 (t, *J* = 6.6 Hz, 2H), 2.90 (t, *J* = 6.2 Hz, 2H), 2.51 (s, 3H), 2.03-1.77 (m, 4H); ^{13}C NMR (100 MHz, $CDCl_3$, ppm) δ: 168.6, 161.9, 152.1, 151.4, 150.2, 148.3, 144.5, 141.0, 136. 9, 134.2, 129.4, 129.0, 128.1, 127.8, 126.2, 125.2, 125.0, 124.62, 124.2, 120.5, 115.9, 59.4, 51.4, 50.8, 50.3, 46.9, 43.0, 34.1, 26.8, 22.8, 22.6. ESI-MS: $C_{32}H_{32}Cl_2N_8O$, Exact Mass: 614.21, m/z 616.4 $(M + 2)^+$.

1-(4-(6-Chloro-1,2,3,4-tetrahydroacridin-9-yl)piperazin-1-yl)-5-(((1-(7-chloroquinolin-4-yl)-1H-1,2,3-triazol-4-yl)methyl)(methyl)amino)pentan-1-one (8b5). Yield: 37%; White solid; mp:127-130°C. ^{1}H NMR (400 MHz, $CDCl_3$, ppm) δ: 9.05 (d, *J* = 4.6 Hz, 1H), 8.23 (d, *J* = 2.0 Hz, 1H), 8.09 (s, 1H), 8.05-8.00 (m, 2H), 7.94 (d, *J* = 2.1 Hz, 1H), 7.59 (dd, *J* = 9.1, 2.1 Hz, 1H), 7.53 (d, *J* = 4.6 Hz, 1H), 7.35 (dd, *J* = 9.0, 2.1 Hz, 1H), 4.09-3.64 (m, 6H), 3.09 (t, *J* = 6.6 Hz, 2H), 2.87 (t, *J* = 6.2 Hz, 2H), 2.59 (t, *J* = 7.0 Hz, 2H), 2.48-2.40 (m, 5H), 1.96-1.66 (m, 8H); ^{13}C NMR (100 MHz, $CDCl_3$, ppm) δ: 171.5, 161.9, 152.1, 151.4, 150.2, 148.3, 145.9, 141.0, 136.8, 134.2, 129.4, 129.0, 128.1, 127.8, 126.1, 125.0, 124.7, 124.60, 124.2, 120.5, 115.9, 56.8, 52.2, 50.7, 50.3, 46.8, 42.7, 42.3, 34.1, 33.1, 27.0, 26.8, 23.0, 22.8, 22.6. ESI-MS: $C_{35}H_{38}Cl_2N_8O$, Exact Mass: 656.25, m/z 657.2 $(M + 1)^+$.

N-(2-((6-Chloro-1,2,3,4-tetrahydroacridin-9-yl)amino)ethyl)-5-(1-(7-chloroquinolin-4-yl)-1H-1,2,3-triazol-4-yl)pentanamide (8b6). Yield: 65%; White solid; mp:112-114 °C. ^{1}H NMR (400 MHz, $CDCl_3$, ppm) δ: 8.98 (d, *J* = 3.9 Hz, 1H), 8.17 (s, 1H), 7.94-7.73 (m, 4H), 7.51-7.31 (m, 3H), 7.11 (d, *J* = 8.5 Hz, 1H), 5.19 (s, 1H), 3.61 (d, *J* = 23.7 Hz, 4H), 3.92-3.33 (m, 8H), 1.80 (s, 8H); ^{13}C NMR (100 MHz, $CDCl_3$, ppm) δ: 174.7, 159.1, 151.3, 150.9, 150.0, 148.3, 147.4, 140.9, 136.7, 134.0, 129.2, 128.8, 126.6, 124.6, 124.6, 124.0, 122.8, 120.4, 117.8, 115.8, 115.4, 50.2, 40.5, 36.0, 33.8, 28.6, 25.1, 25.0, 22.9, 22.5. ESI-MS: $C_{31}H_{31}Cl_2N_7O$, Exact Mass: 587.20, m/z 589.0 $(M + 2)^+$.

Acetylcholinesterase and Butyrylcholinesterase Inhibition Assay.

View Article Online
DOI: 10.1039/C7MD00457E

The inhibition ability of tacrine-derivatives **8a1-8a5** and **8b1-8b6** for electric eel acetylcholinesterase (eeAChE; Sigma-Aldrich, USA; Enzyme Information Download Website: https://www.sigmaaldrich.com/content/dam/sigma-aldrich/docs/Sigma/Product_Information_Sheet/c3389pis.pdf) and horse serum butyrylcholinesterase (hsBChE; Sigma-Aldrich, USA; Enzyme Information Download Website: https://www.sigmaaldrich.com/content/dam/sigma-aldrich/docs/Sigma/Datasheet/c1057dat.pdf) were tested using the 5,5'-dithiobis-(2-nitrobenzoic acid) (DTNB) method with the related assay kit (Keygen, China). DTNB would generate 5-mercapto-2-nitrobenzoic acid-a detectable chromophore at the 405-412 nm range. The final concentrations (100 μM, 20 μM, 4 μM, 0.8 μM, 0.16 μM, 0.032 μM) of screening compounds were prepared using DMSO. In 96-well plates, 20 μL eeAChE (or hsBChE, 0.5 u/mL diluted using saline) was incubated with above different concentrations test compounds at room temperature for 15 min followed by the addition of relative agents according to the kit instruction. Finally, the chromophore absorbance was examined at the wavelength of 405 nm *via* microplate reader (Thermo MK3). Percentage of inhibition was calculated by the comparison of compound-treated to various control incubations.**Molecular simulations**

Preparation of hAChE/hBChE structures and ligands

The atomic coordinates of the hAChE and hBChE were obtained from the Protein Data Bank (PDB ID: hAChE: 1B41 (resolution 2.76 Å)[40] and hBChE: 1P0I (resolution 2.0 Å).[41] Protein structures were imported into the Maestro module available in the Schrödinger Suite (Schrödinger, LLC) [42] and subsequently, both structures were optimized separately by using the Protein Preparation Wizard.[43] This protein structure optimization includes adding hydrogen atoms, assigning bond orders and building disulfide bonds. The protonation states of the ionisable residues (pH = 7) were predicted by the PROPKA tool provided in the Protein Preparation Wizard.[41] An optimized structure was finally found by energy minimization (i.e., position of the hydrogen atoms) with the OPLS_2005 force field.

The 3D structures of **8a2** and Tacrine were built with Maestro and preprocessed using the LigPrep module (v2.5)[44] of the Schrödinger modeling software. Preprocessing includes Energy minimization using the OPLS_2005 force field and determination of ionization states at pH = 7 (+/-2).[45]

Molecular docking simulation

View Article Online
DOI: 10.1039/C7MD00457E

The receptor grid generation module of Glide [46] was used to define both peripheral site (PAS) and catalytic sites (CAS) for the docking experiments in hAChE and hBChE. A set of PAS and CAS residues was as the centroid of the grid box (of size 20 Å).[40,41] Water molecules at the active site were deleted. Glide uses an in-build docking scoring function resulting in a Glidescore (Standard Precision). The docking and scoring function parameters and settings used in this study are described in detail elsewhere.[47] The best 25 docking solutions for each protein structure were selected for investigation, followed by MM-GBSA calculation.[48-50] The Prime MM-GBSA method calculates the binding affinity of the ligand (ΔG_{bind}) by energy minimization procedures. The binding energy of the ligand was extracted from an energy-optimized protein-ligand complex and Prime MM-GBSA by using the VSGB 2.0 solvation (implicit) model.[51,50] During binding affinity calculation, the program offers the option to treat the ligand and protein as flexible; in this study, a 5Å region of the protein around the ligand was treated as flexible.

Conflict of Interest

The authors declare no conflict of interests.

Ethical Statement

All procedures were conducted in strict accordance with the Chinese relevant laws and institutional guidelines (School of Pharmaceutical Sciences, Shandong University).This study was performed in strict accordance with the NIH guidelines for the care and use of laboratory animals (NIH Publication No. 85-23 Rev. 1985) and was approved by the Institutional Animal Care and Use Committee of Shandong University (Shandong, China)".

Acknowledgements

Financial support from the Key Research and Development plan of Shandong Province (No. 2017CXGC1401), Major Project of Science and Technology of Shandong Province (No. 2015ZDJS04001) is gratefully acknowledged.

Author Contributions

The manuscript was written through contributions of all authors. All authors have given approval to the final version of the manuscript.

View Article Online
DOI: 10.1039/C7MD00457E

References

1. D. M. Walsh and D. J. Selkoe, *Neuron*, 2004, 44, 181-193.

2. A. Wimo, L. Jönsson, J. Bond, M. Prince and B. Winblad, *Alzheimers Dement.*, 2013, 9, 1-11.e13.

3. A. Wimo, M. Guerchet, G. C. Ali, Y. T. Wu, A. M. Prina, B. Winblad, L. Jönsson, Z. Liu and M. Prince, *Alzheimers Dement.*, 2016, 13, 1-7.

4. P. D. Sloane, S. Zimmerman, C. Suchindran, P. Reed, L. Wang, M. Boustani and S. Sudha, *Annu. Rev. Public Health,* 2002, 23, 213-31.

5. X. Zha, D. Lamba, L. Zhang, Y. Lou, C. Xu, D. Kang, L. Chen, Y. Xu, L. Zhang, A. De Simone, S. Samez, A. Pesaresi, J. Stojan, M. G. Lopez, J. Egea, V. Andrisano and M. Bartolini, *J Med Chem*, 2016, 59, 114-131.

6. A. Enz, R. Amstutz, H. Boddeke, G. Gmelin and J. Malanowski, *Prog. Brain. Res.,* 1993, 98, 431-438.

7. P. Davies and A. J. Maloney, *Lancet*, 1976, 2, 1403.

8. M. A. Babu, M. Lakshmi, P. Vasanthanathan and S. G. Kaskhedikar, *Indian J Pharm Sci.* 2005, 67, 1-10.

9. M. Weinstock, *Cns Drugs*, 1999, 12, 307-323.

10. N. H. Greig, T. Utsuki, D. K. Ingram, Y. Wang, G. Pepeu, Q. S. Yu, K. Furukawa, K. Sambamurti, A. Brossi and D. K. Lahiri, *Natl. Acad. Sci. USA,* 2005, 102, 17213-17218.

11. S. Darvesh, D. A. Hopkins and C. Geula, *Nat. Rev. Neurosci.* 2003, 4, 131-138.

12. R. M. Lane, S. G. Potkin and A. Enz, *Int. J Neuropsychopharmacol.,* 2006, 9, 101-124.

View Article Online
DOI: 10.1039/C7MD00457E

13. D. C. Vellom, Z. Radić, Y. Li, N. A. Pickering, S. Camp and P. Taylor, *Biochemistry*, 1993, 32, 12-17.

14. F. B. M. Isabel, P. Concepción, C. N. Eugenia, P. J. Antonio, U. Paola, G. P. Esther, L. Manuela G, V. Mercedes and G. Antonio G, *Chemmedchem*, 2010, 4, 828-841.

15. V. Tumiatti, A. Minarini, M. L. Bolognesi, A. Milelli, M. Rosini and C. Melchiorre, *Curr. Med. Chem.,* 2010, 17, 1825-1838.

16. P. B. Watkins, H. J. Zimmerman, M. J. Knapp, S. I. Gracon and K. W. Lewis, *Jama*, 1994, 271, 992-998.

17. P. R. Carlier, E. S. Chow, Y. Han, J. Liu, Y. J. El and Y. P. Pang, *J. Med. Chem.,* 1999, 42, 4225-4231.

18. M. I. Fernándezbachiller, C. Pérez, G. C. Gonzálezmuñoz, S. Conde, M. G. López, M. Villarroya, A. G. García and M. I. Rodríguezfranco, *J. Med. Chem.,* 2010, 53, 4927-4937.

19. H. Zheng, M. Fridkin and M. Youdim, *Pharmaceuticals*, 2014, 7, 113-115.

20. X. Q. Wang, C. L. Xia, S. B. Chen, J. H. Tan, T. M. Ou, S. L. Huang, D. Li, L. Q. Gu and Z. S. Huang, *Eur. J. Med. Chem.,* 2015, 89, 349-361.

21. S. G. Agalave, S. R. Maujan and V. S. Pore, *Chem. Asian J.,* 2011, 6, 2696-2718.

22. X. Wang, B. Huang, X. Liu and P. Zhan, *Drug Discov. Today,* 2016, 21, 118-132.

23. P. Gao, L. Sun, J. Zhou, X. Li, P. Zhan and X. Liu, *Expert Opin. Drug Discov.,* 2016, 11, 857-871.

24. C. Wang, D. Ikhlef, S. Kahlal, J. Y. Saillard and D. Astruc, *Coord. Chem. Rev.,* 2016, 316, 1-20.

View Article Online
DOI: 10.1039/C7MD00457E

25. E. Ö. Özer, O. U. Tan, K. Ozadali, T. Küçükkılınç, A. Balkan and G. Uçar, *Bioorg. Med. Chem. Lett.,* 2013, 23, 440.

26. S. Ariyasu, A. Sawa, A. Morita, K. Hanaya, M. Hoshi, I. Takahashi, B. Wang and S. Aoki, *Bioorg. Med. Chem.,* 2014, 22, 3891-3905.

27. L. Guetzoyan, F. Ramiandrasoa, H. Dorizon, C. Desprez, A. Bridoux, C. Rogier, B. Pradines and M. Perrée-Fauvet, *Bioorg. Med. Chem.,* 2007, 15, 3278-3289.

28. R. Musiol, J. Jampilek, J. E. Nycz, M. Pesko, J. Carroll, K. Kralova, M. Vejsova, J. O'Mahony, A. Coffey and A. Mrozek, *Molecules*, 2010, 15, 288-304.

29. J. J. Bornstein, T. J. Eckroat, J. L. Houghton, C. K. Jones, K. D. Green and S. Garneau-Tsodikova, *Medchemcommun*, 2011, 2, 406-412.

30. J. A. González-Vera, E. Luković and B. Imperiali, *J. Org. Chem.,* 2009, 74, 7309-7314.

31. J. Zhao and Q. Zhu, *Bioorg. Med. Chem. Lett.,* 2010, 20, 6222-6225.

32. T. Mohamed and P. P. Rao, *Bioorg. Med. Chem. Lett.,* 2010, 20, 3606-3609.

33. T. Mohamed, J. C. K. Yeung, M. S. Vasefi, M. A. Beazely and P. P. N. Rao, *Bioorg. Med. Chem. Lett.,* 2012, 22, 4707-4712.

34. G. L. Ellman, K. D. Courtney, A. V. Jr and R. M. Feather-Stone, *Biochem. Pharmacol.,*, 1961, 7, 88-95.

35. G. Tin, T. Mohamed, N. Gondora, M. A. Beazely and P. P. N. Rao, *Medchemcomm*, 2015, 6, 1930-1941.

36. I. Khan, S. Bakht, A. Ibrar, S. Abbas, S. Hameed, J. White, U. Rana, S. Zaib, M. Shahid and J. Iqbal, *Rsc Advances*, 2015, 5, 21249-21267.

37. M. Harel, I. Schalk, L. Ehret-Sabatier, F. Bouet, M. Goeldner, C. Hirth, P. H. Axelsen, I.

View Article Online
DOI: 10.1039/C7MD00457E

Silman and J. L. Sussman, *Proc. Natl. Acad. Sci. USA,* 1993, 90, 9031-9035.

38. M. I. Fernandez-Bachiller, C. Perez, N. E. Campillo, J. A. Paez, G. C. Gonzalez-Munoz, P. Usan, E. Garcia-Palomero, M. G. Lopez, M. Villarroya, A. G. Garcia, A. Martinez and M. I. Rodriguez-Franco, *ChemMedChem*, 2009, 4, 828-841.

39. A. Milelli, S. A. De, N. Ticchi, H. H. Chen, N. Betari, V. Andrisano and V. Tumiatti, *Curr. Med. Chem.*, 2017, 24.

40. G. Kryger, M. Harel, K. Giles, L. Toker, B. Velan, A. Lazar, C. Kronman, D. Barak, N. Ariel, A. Shafferman, I. Silman and J. L. Sussman, *Acta crystallographica. Section D, Biol. Crystallogr.,* 2000, 56, 1385-1394.

41. Y. Nicolet, O. Lockridge, P. Masson, J. C. Fontecilla-Camps and F. Nachon, *J. Biol. Chem.,* 2003, 278, 41141-41147.

42. Maestro, *Schrödinger,* , LLC, New York, NY, 2015.

43. G. M. Sastry, M. Adzhigirey, T. Day, R. Annabhimoju and W. Sherman, *J. Comput. Aided Mol. Des.,* 2013, 27, 221-234.

44. LigPrep, Schrödinger, LLC, New York, NY, 2015.

45. Epik, Schrödinger, LLC, New York, NY, 2015.

46. R. A. Friesner, J. L. Banks, R. B. Murphy, T. A. Halgren, J. J. Klicic, D. T. Mainz, M. P. Repasky, E. H. Knoll, M. Shelley, J. K. Perry, D. E. Shaw, P. Francis and P. S. Shenkin, *J. Med. Chem.,* 2004, 47, 1739-1749.

47. V. Poongavanam and J. Kongsted, *PloS one*, 2013, 8, e73478.

48. Prime, Schrödinger, LLC, New York, NY, 2015.

49. S. Genheden and U. Ryde, *Expert Opin. Drug Discov.,* 2015, 10, 449-461.

View Article Online
DOI: 10.1039/C7MD00457E

50. P. A. Greenidge, C. Kramer, J. C. Mozziconacci and R. M. Wolf, *J. Chem. Inf. Model.,* 2013, 53, 201-209.

51. J. Li, R. Abel, K. Zhu, Y. Cao, S. Zhao and R. A. Friesner, *Proteins*, 2011, 79, 2794-2812.